34th Annual International Conference of the IEEE EMBS
San Diego, California USA, 28 August - 1 September, 2012

Performance of Beamformers on EEG Source Reconstruction

Yaqub Jon Mohamadi, Govinda Poudel, *Member, IEEE*, Carrie Innes, Richard D. Jones, *Senior Member, IEEE*

Abstract— **Recently a number of new beamformers have been introduced for reconstruction and localization of neural sources from EEG and MEG. However, little is known about the relative performance of these beamformers. In this study, 8 scalar beamformers were examined with respect to several parameters to determine how effective they are at reconstruction of a dipole time course from EEG. A simulated EEG signal was produced by means of forward head modelling for projection of an artificial dipole on scalp electrodes then superimposed on background signal. Both real EEG and white noise were applied as background activity. Although the eigenspace beamformer can perform slightly better than other beamformers for small dipoles, and even more so for large dipoles, it is not a contender for real-time beamforming of EEG as it cannot be completely automated. Overall, in terms of performance, robustness to variations in parameters, and ease of application, the minimum variance and Borgiotti-Kaplan beamformers were found to be the best performers.**

I. Introduction

In recent years, new beamformers have been introduced for brain source localization and reconstruction from EEG and MEG [1-4]. The beamformer provides a versatile form of spatial filtering suitable for processing data from an array of sensors [1]. Beamformers were originally applied in array signal processing including sonar, radar and seismic exploration [5]. A beamformer in EEG and MEG is a spatial filter applied to any location in the brain and by attenuating the effects of sources from all other locations, the beamformer allows us to estimate the source at that particular spatial location from a segment of EEG [6].

Beamformers applied to EEG or MEG fall into two main categories: (A) scalar beamformer for which the orientation of the dipole is known or assumed and (B) vector beamformers which reconstruct the dipole time course in 3 orthogonal directions and does not require knowledge of the dipole orientation in advance. For this study, 8 scalar beamformers were evaluated: (1) minimum variance (MV), (2) generalized side lobe canceller form of minimum variance (GSC) [7], (3) weight normalized minimum variance (WNMV) [3], (4) standardized minimum variance (SMV) [3], (5) Borgiotti-Kaplan (BK) [8], (6) eigenspace extension of the minimum variance (ESMV), (7) array-gain constraint minimum-norm with recursively updated Gram matrix (AGCMN) [4], and (8) higher order covariance matrix of minimum variance (HOC) [2].

In this study we used numerical simulation to evaluate the performance of beamformers for the reconstruction of a known dipole time course when depth, magnitude, position, orientation, interference, and background signal are varied.

Throughout this paper, plain italics indicate scalars, lower case boldface italics indicate vectors, and upper case boldface italics indicate matrices.

Manuscript received June 2, 2012.

Y. Jon Mohamadi is a PhD student in the Department of Medicine, University of Otago, Christchurch, New Zealand (e-mail: jonya247@student.otago.ac.nz).

R. D. Jones is with the Department of Medical Physics and Bioengineering, Christchurch Hospital, and Department of Medicine, University of Otago, and Department of Electrical & Computer Engineering, University of Canterbury, and New Zealand Brain Research Institute, Christchurch, New Zealand (e-mail: richard.jones@nzbri.org).

G. Poudel was with the New Zealand Brain Research Institute, Christchurch, New Zealand and is now with Monash Biomedical Imaging, Monash University, Melbourne, Australia (e-mail: govinda.poudel@monash.edu).

C. R. H. Innes is with the Department of Medical Physics and Bioengineering, Christchurch Hospital, and New Zealand Brain Research Institute, Christchurch 8011, New Zealand (e-mail: carrie.innes@nzbri.org).

II. Methods

A. Forward problem

The simulated EEG signals on M electrodes at time t are $\boldsymbol{b}(t) = [b_1(t), b_2(t), \dots, b_M(t)]$ where

$$\boldsymbol{b}(t) = \begin{cases} \boldsymbol{n}(t), & t = 0, \dots, \frac{N}{2} - 1 \\ (\boldsymbol{L}(\boldsymbol{r}_d)\boldsymbol{q})s(t) + \boldsymbol{n}(t), & t = \frac{N}{2}, \dots, N-1 \end{cases} \quad (1)$$

where $N = 15000$, is the number of time samples $\boldsymbol{L}(\boldsymbol{r}_d) = [\boldsymbol{l}_x(\boldsymbol{r}_d), \boldsymbol{l}_y(\boldsymbol{r}_d), \boldsymbol{l}_z(\boldsymbol{r}_d)]$ is a $M \times 3$ leadfield matrix which shows the sensitivity of M EEG electrodes for a dipole located at $\boldsymbol{r}_d = [r_{dx}, r_{dy}, r_{dz}]^T$ (mm) in the head, $\boldsymbol{q} = \alpha \boldsymbol{q}_d$ is the dipole moment in A-m, $\boldsymbol{q}_d = [q_{dx}, q_{dy}, q_{dz}]^T$ is the normalized dipole orientation for which $|\boldsymbol{q}_d| = 1$, α is the dipole magnitude, $s(t)$ is the dipole time course with normalized magnitude, and $\boldsymbol{n}(t)$ is the additive background signal which can be white noise or real EEG. In this study, a sinusoidal signal was used as the dipole time course

$$s(t) = \sin(2\pi f t) \quad (2)$$

where f is the dipole frequency, $f = 10$ Hz. The normalized leadfield ($\boldsymbol{L}/\|\boldsymbol{L}\|$) was used for this study.

B. Beamformer

The reconstructed dipole time course from the EEG for a scalar beamformer is

$$\hat{s}(t) = \boldsymbol{w}(\boldsymbol{r}_b, \boldsymbol{q}_b)\boldsymbol{b}(t), \quad (3)$$

where $\boldsymbol{r}_b$ and $\boldsymbol{q}_b$ are the estimated dipole location and orientation respectively for calculation of the beamformer

weight and $\boldsymbol{w}(\boldsymbol{r}_b, \boldsymbol{q}_b)$ is weight vector for the scalar beamformer

$$\boldsymbol{w}(\boldsymbol{r}_b, \boldsymbol{q}_b) = \left[\boldsymbol{w}_x(\boldsymbol{r}_b, \boldsymbol{q}_b), \boldsymbol{w}_y(\boldsymbol{r}_b, \boldsymbol{q}_b), \boldsymbol{w}_z(\boldsymbol{r}_b, \boldsymbol{q}_b)\right]. \quad (4)$$

The covariance matrix is calculated from

$$\boldsymbol{C} = \langle \boldsymbol{b}(t)\boldsymbol{b}(t)^T \rangle, \quad (5)$$

where $\langle . \rangle$ is the ensemble average.

C. Performance measures

Performance of the beamformers was estimated by signal-to-noise ratio of the output ($SNRout$) and enhancement ratio (ER). All of the power measures P were calculated over the last 30 s of $\boldsymbol{b}(t)$ by FFT.

$SNRin$ is the ratio of the summation of the power of the dipole on input channels, Pin_d, divided by the summation of the power of background signal on the input channels, Pin_n:

$$SNRin = \frac{\sum_{i=1}^{M} Pchan(i)_d}{\sum_{i=1}^{M} Pchan(i)_n} = \frac{Pin_d}{Pin_n} \quad (6)$$

where Pin_d is the power of $(\boldsymbol{L}(\boldsymbol{r}_d)\boldsymbol{q})s(t)$ and Pin_n is the power of $\boldsymbol{n}(t)$ for a given time window. In the ideal case, $SNRin$ does not depend on dipole location and orientation, $\boldsymbol{r}_d$ and $\boldsymbol{q}_d$, and depends only on dipole magnitude α. Based on our simulations, $SNRin$ can change slightly with variation in dipole location and orientation.

$SNRout$ is the output power of the beamformer at the frequency of the dipole, $Pout_{10\,Hz}$, divided by the total power of the beamformer output less the power at the frequency of the dipole

$$SNRout = \frac{Pout_{10\,Hz}}{Pout_{total} - Pout_{10\,Hz}}. \quad (7)$$

Although there are simpler methods to compute $SNRin$, such as Frobenius norm of the signal matrix to that of the noise matrix, we cannot compute $SNRout$ by this method as the signal and noise on the output are not available in separate matrices.

$SNRin_{MAX}$ is the highest SNR at any electrode found by dividing the power of the dipole at each input channel ($Pchan(i)_d$, i is channel 1, 2, ... 64 in the EEG 10-20 system) by the power of the background signal in the same channel ($Pchan(i)_n$)

$$SNRin_{MAX} = MAX\left[\frac{Pchan(i)_d}{Pchan(i)_n}\right], i = 1, 2, \ldots, M. \quad (8)$$

The enhancement ratio ER is then defined as

$$ER = \frac{SNRout}{SNRin_{MAX}}. \quad (9)$$

III. Computer simulations

A. Simulated EEG signal

60 s of EEG signal was simulated by means of a 30 s sinusoidal signal (10 Hz) projected on the scalp via forward head modelling and superimposed on the background signal (real EEG or white noise). The first 30 s of the simulated EEG signal is only the background signal, $\boldsymbol{n}(t)$. The boundary element method (BEM) model of the head [9] from an averaged MRI data set (Montreal Neurological Institute), implemented in the FieldTrip toolbox [10], was used for the forward solution. The real EEG data used as additive background signal in this study was obtained from an earlier study of healthy subjects [11]. The mapping standard 10-20 system was used to define the location of the 64 electrodes and the reference electrode was between the CZ and CPZ electrodes.

B. Parameters for evaluation of the beamformers

(1) Depth of dipole

To assess the effect of depth of dipole on beamformer performance, the dipole moment $\boldsymbol{q}$ was fixed, while the dipole depth was varied. For this experiment, depth is the distance of the dipole from a scalp point close to the ear at MNI coordinate [84, -35, 0](mm), and the dipole moved from the right ear towards the left ear.

(2) Dipole magnitude

To assess the effect of varying dipole magnitudes on beamformer performance, the position $\boldsymbol{q}_d$ and orientation $\boldsymbol{r}_d$ of the dipole were fixed, while different magnitudes α were assigned to the dipole.

(3) Misestimation of dipole position

The ideal is for the position of the beamformer, $\boldsymbol{r}_b$ where $\boldsymbol{r}_b = \left[r_{bx}, r_{by}, r_{bz}\right]^T$(mm), to be the same as that of the dipole, $\boldsymbol{r}_d$. However, in practice, the exact location of the dipole is not known in advance, i.e., $\boldsymbol{r}_b \neq \boldsymbol{r}_d$. For this investigation, beamformers were run at increasing distances from the actual location of the dipole.

(4) Misestimation of dipole orientation

For scalar beamformers, an estimate of the orientation of the dipole needs to be given, with incorrect estimation leading to degraded performance of the beamformer. The beamformer output power is maximum when the estimated dipole orientation applied in the beamformer is equal to the actual orientation of the dipole, i.e., $\boldsymbol{q}_b = \boldsymbol{q}_d$ [12], where $\boldsymbol{q}_b = \left[q_{bx}, q_{by}, q_{bz}\right]^T$ is the estimated dipole orientation and $|\boldsymbol{q}_b| = 1$. For this part, while the $\boldsymbol{q}_d$ stayed constant, different values of $\boldsymbol{q}_b$ were applied for beamformers to see how sensitive beamformers are to misestimation of dipole orientation.

(5) Interference from another dipole source signal

To assess the effect of interference, a second dipole source (10.4 Hz) was placed at different distances (0 to 18 mm) from the original dipole (10 Hz), and also superimposed on the background signal. The power of the beamformer output was measured at the frequency of the

dipole of interest and that of interfering dipole. The signal-to-interference ratio (SIR) is defined as

$$SIR = \frac{Pout_{10\,Hz}}{Pout_{10.4\,Hz}}. \quad (10)$$

(6) Additive background signal

To assess the effect of different types of additive background signal $\boldsymbol{n}(t)$, two types of background signal were superimposed on the dipole signal: white noise and real EEG. EEG data from five subjects were used to determine differences in beamformer performance between different EEGs and even white noise. The use of real EEG data as additive background signal is also reported in [13] and [7]. Most of the signals picked up by EEG or MEG are produced by simultaneous activation of tens of thousands of neurons [14] acting coherently in the cortical gray matter [15]. Consequently, when real EEG was used as additive background we put the dipole in the white matter (except in the experiment where we were assessing the effect of dipole depth). This helped ensure that background activity appearing in the beamformer output was not coming from the same place as the dipole. In Fig. 1 to 5, real EEG from subject 102 was used as additive background signal.

IV. Results

(1) Depth of dipole

When a dipole was moved from a cortical to a deeper (change in $\boldsymbol{r}_d$), the $SNRout$ of all beamformers decreased but not nearly as much as $SNRin_{MAX}$. Hence, ER increases with depth of dipole (Fig. 1). That is, beamformers are better able to reconstruct electrical activity from cortical dipoles but, conversely, deeper signals are enhanced more.

(2) Dipole magnitude

It is clear that beamformers are non-linear and better able to enhance small dipole signals (Fig. 2).

(3) Misestimation of dipole position

Most of the beamformers had similar behaviour to each other when misestimating the dipole position (Fig. 3). The drop off in ER with separation of beamformer and dipole is, however, also dependent on the depth of the dipole. For deeper dipoles, misestimation of dipole position caused much less drop in the beamformer $SNRout$ than for cortical dipoles.

(4) Misestimation of dipole orientation

The SMV beamformer was the most sensitive to misestimation of dipole orientation, with a small difference between the estimated orientation and the actual orientation of the dipole considerably degrading the performance of this beamformer (Fig. 4).

(5) Interference from another dipole source signal

Most of the beamformers have similar behaviour when interfered with by another dipole source. Fig. 5 shows the behaviour of the beamformers for an interfering dipole.

(6) Additive background signal

The AGCMN beamformer performed well when white noise was applied; but, when real EEG was used as additive

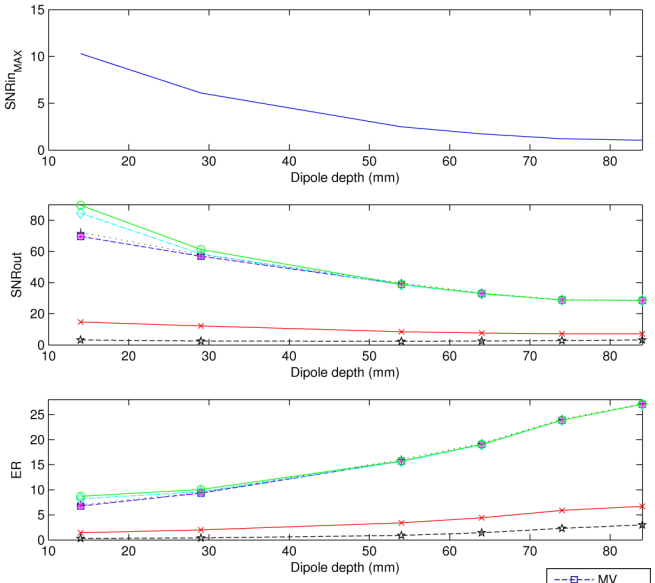

Fig. 1. The effect of dipole depth inside the brain on the performance of the beamformers for a dipole with orientation [1 0 0] while dipole magnitude and orientation are fixed, $SNRin$=0.33.

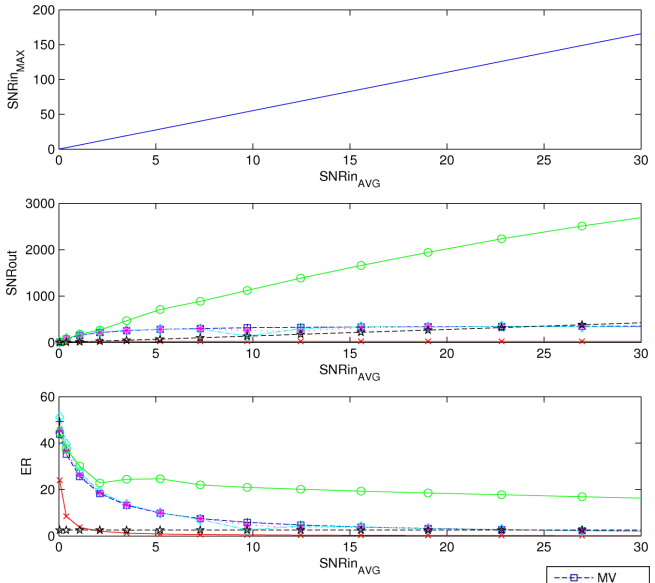

Fig. 2. The effect of varying the magnitude of the dipole on the performance of beamformers for a dipole located at [22, 38, 0](mm) and orientation [-0.5, 0.6, 0.6].

background, this beamformer performed poorly. The ESMV beamformer also had a better performance when white additive background signal was used than when real EEG was used.

The two main differences between white noise and real EEG are: (1) in white noise all the frequency components have similar power opposed to real EEG and, (2) there is no correlation between channels for white noise while in real EEG there is some correlation between signals of different channels (spatially non-white). It is also shown in [16] that real EEG as additive background signal introduces a

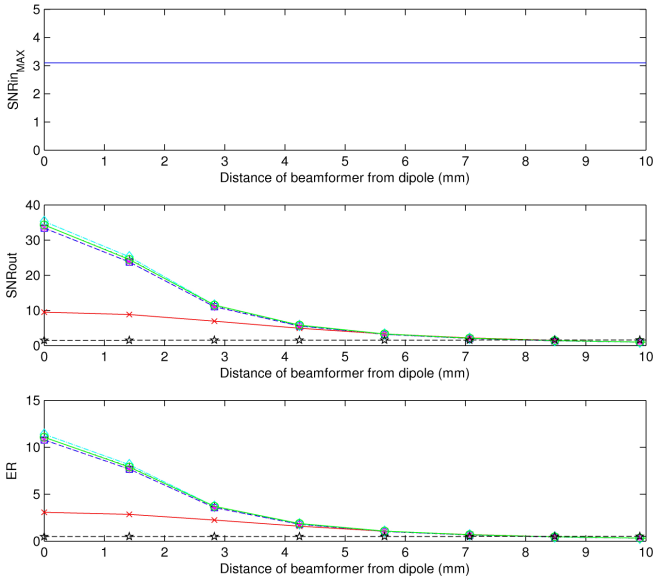

Fig. 3. The effect of misestimation of dipole position on the performance of beamformers for a dipole located at [24, 42, 0](mm), orientation [0.33 0.66 0.66], fixed magnitude, $SNRin$= 0.37. In the first sample point, the location given to the beamformer is exactly the location of the dipole source signal, $\boldsymbol{r}_b = \boldsymbol{r}_d$, while for other sample points the location given to the beamformer becomes farther and farther from the dipole source signal.

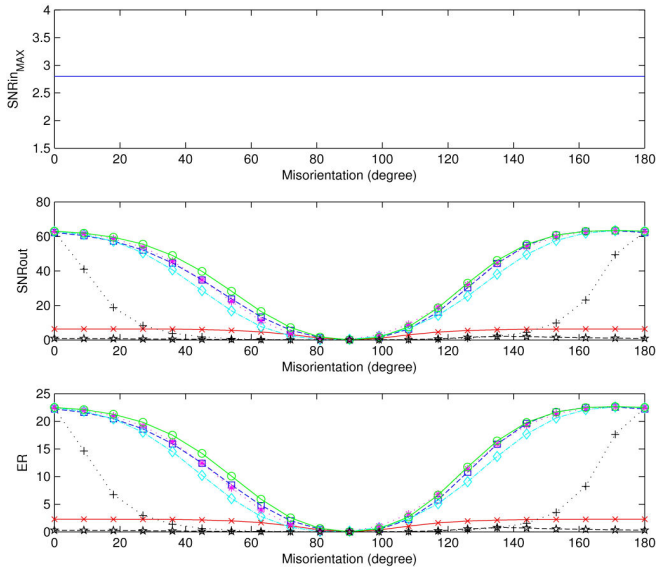

Fig. 4. The effect of misestimation of dipole orientation on the performance of beamformers for a dipole located at [25, -54, 26](mm) orientation [0, 0.7, 0.7] and fixed magnitudes, $SNRin$=0.2. For each sample, the estimated dipole orientation given to the beamformer is different, to some extent, in the first sample point $\boldsymbol{q}_b = \boldsymbol{q}_d$ and for the rest of the sample points q_{by}, q_{bz} changed while $q_{bx} = 0$. The last sample point $\boldsymbol{q}_b = [0, -0.7, -0.7]$ corresponds to 180 deg misestimation of dipole orientation.

spatially non-uniform component to the neural power map that depends on the measurement site. Also, by applying EEG of different subjects as additive background, we found that SMV and WNMV are less robust to changes in the background EEG.

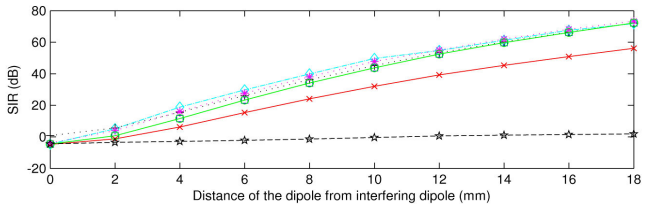

Fig. 5. The SIR for a moving interfering dipole with a fixed orientation [0, 0.83, 0.51] and magnitude in all locations while the dipole of interest had a fixed location of [28, -20, 34] (mm), magnitude, and orientation [-0.33, 0.67, 0.67]. $SNRin$=0.8.

V. Discussion

(1) Minimum variance (MV)

The MV beamformer proved to be reliable throughout this study as its performance was less sensitive to changes in the different parameters. The MV beamformer also has the simplest formulation for weight calculation and needs less computational effort than the other beamformers.

(2) Borgiotti-Kaplan (BK)

The BK was found to perform very similarly to the MV beamformer in our study.

(3) Generalized side lobe canceller form of minimum variance (GSC)

The GSC performed poorly compared to most other beamformers. The only situation in which it performed acceptably was when $SNRin$ was low. As the magnitude of the dipole increases the $SNRout$ of this beamformer dropped dramatically. The reason for this drop is that this beamformer has two channels, one a fixed (quiescent) beamformer and the other a blocking channel which includes a blocking matrix and an adaptive filter which has a feedback loop. Some of the reconstructed signal $\hat{s}(t)$ is fed to the blocking matrix through this feedback loop and is subtracted from the scalar beamformer output which degrades the $SNRout$. Computational effort needed due to adaptive updates for each time sample is another disadvantage of GSC.

(4) Eigenspace extension of minimum variance (ESMV)

The ESMV is an effective beamformer when the $SNRin$ is high but otherwise performs only slightly better or the same as the MV beamformer (Fig. 2). The reason is that when the $SNRin$ is high the signal space is small and noise space is large, by removing the noise space by means of eigenvalue decomposition of the covariance matrix a substantial amount of noise disappears from the beamformer output and the $SNRout$ increases. However, when the $SNRin$ is low, the noise space is small and, as a result, removing the noise space makes little change to $SNRout$. In [1], where the eigenspace extension of the vector BK beamformer was proposed and compared with the vector MV beamformer, it is mentioned that for the simulations, high $SNRin$ values were applied which means the result of the comparison could be different if $SNRin$ was lower. The ESMV beamformer also had a better performance when white noise was used as the additive background signal

rather than real EEG. Although the solution proposed in [17] is a form of prewhitened extension of the ESMV beamformer for non-white noise, the covariance matrix for the prestimuli signals needed to be defined separately. Consequently, the ESMV beamformer has been found to be more useful for evoked potentials [18].

Furthermore, a serious deficiency of the ESMV beamformer is that it needs user information to determine the size of the signal and noise spaces, which cannot be automated.

The ESMV beamformer exhibited marginally better performance than the other beamformers in reconstruction of more cortical source signals (Fig. 1) as cortical source signals are spatially more separable than deep EEG sources [17].

(5) Weight normalized minimum variance (WNMV)

The WNMV beamformer was found to be overly sensitive to the EEG background signal. In addition, Greenblatt et al. [3] reported that the WNMV beamformer is sensitive to dipole magnitude.

(6) Standardized minimum variance (SMV)

The SMV beamformer was found to have a similar performance to WNMV. The SMV was also very sensitive to misestimation of the dipole orientation, Fig. 4.

(7) Array-gain constraint minimum norm spatial filter with recursively updated Gram matrix (AGCMN)

The AGCMN beamformer has been recently introduced [4] and works well when white noise is used as additive background signal. However, when real EEG is used it performs very poorly, except for high $SNRin$ (e.g., $SNRin = 16$ in [4]). Thus, this beamformer is well-suited to study neural responses to evoked stimulation, but not for studying brain activities that are not time-locked to stimuli [19]. The plots of $SNRout$ and ER in Fig. 2 show that the AGCMN beamformer performs better than the MV beamformer only when the $SNRin \geq 25$. Another big disadvantage is the huge computational effort needed as the weights have to be updated for each time sample.

(8) Higher-order covariance extension of MV (HOC)

The HOC was unable to reconstruct the dipole time course under any condition (and, hence, was omitted in Figs 1-5). In fact, there was no example in the original paper [2] of time course reconstruction by this beamformer, as it was only compared to other beamformers in terms of neural activity index.

VI. Conclusion

Although the ESVM beamformer can perform slightly better than other beamformers for small dipoles, and even more so for large dipoles, it is not a contender for real-time beamforming of EEG as it cannot be completely automated. Overall, in terms of performance, robustness to variations in parameters, and ease of application, MV and BK beamformers are the best performers.

References

[1] K. Sekihara, S. S. Nagarajan, D. Poeppel, A. Marantz, and Y. Miyashita, "Reconstructing spatio-temporal activities of neural sources using an MEG vector beamformer technique," *IEEE Trans. Biomed. Eng.*, vol. 48, pp. 760-771, 2001.

[2] M. X. Huang, J. J. Shih, R. R. Lee, D. L. Harrington, R. J. Thoma*, et al.*, "Commonalities and differences among vectorized beamformers in electromagnetic source imaging," *Brain Topogr.*, vol. 16, pp. 139-158, 2004.

[3] R. E. Greenblatt, A. Ossadtchi, and M. E. Pflieger, "Local linear estimators for the linear bioelectromagnetic inverse problem," *IEEE Trans. Biomed. Eng.*, vol. 53, pp. 3403-3412, 2005.

[4] I. Kumihashi and K. Sekihara, "Array-gain constraint minimum-norm spatial filter with recursively updated gram matrix for biomagnetic source imaging," *IEEE Trans. Biomed. Eng.*, vol. 57, pp. 1358-1365, 2010.

[5] B. D. Van Veen and K. M. Buckley, "Beamforming: a versatile approach to spatial filtering," *IEEE Acoust., Speech, Signal. Process. Mag.*, vol. 5, pp. 4-24, 1988.

[6] H. V. Dang, K. T. Ng, and J. K. Kroger, "Novel beamformers for multiple correlated brain source localization and reconstruction," *IEEE Int. Conf. Acoust. Speech Sig. Proc.*, vol. 2011, pp. 721-724, 2011.

[7] M. E. Spencer, R. M. Leahy, J. C. Mosher, and P. S. Lewis, "Adaptive filters for monitoring localized brain activity from surface potential time series," *IEEE Proc. Asilomar Conf. Sig. Sys. Comp.*, vol. 26, pp. 156-160, 1992.

[8] G. V. Borgiotti and L. J. Kaplan, "Superresolution of uncorrelated interference sources by using adaptive array techniques," *IEEE Trans. Antennas Propag.*, vol. AP-27, pp. 842-845, 1979.

[9] T. F. Oostendorp and A. van Oosterom, "Source parameter estimation in inhomogeneous volume conductors of arbitrary shape," *IEEE Trans. Biomed. Eng.*, vol. 36, pp. 382-391, 1989.

[10] R. Oostenveld, P. Fries, E. Maris, and J. M. Schoffelen, "FieldTrip: Open source software for advanced analysis of MEG, EEG, and invasive electrophysiological data," *Comput. Intell. Neurosci.*, vol. 2011, pp. 1-9, 2011.

[11] G. R. Poudel, R. D. Jones, C. R. H. Innes, and P. J. Bones, "Characteristics and EEG spectral dynamics of behavioural microsleeps in a mock-MRI scanner," *NeuroImage*, vol. 41, pp. S59, 2008.

[12] K. Sekihara, S. S. Nagarajan, D. Poeppel, and A. Marantz, "Asymptotic SNR of scalar and vector minimum-variance beamformers for neuromagnetic source reconstruction," *IEEE Trans. Biomed. Eng.*, vol. 51, pp. 1726-1734, 2004.

[13] D. M. Ward, R. D. Jones, P. J. Bones, and G. J. Carroll, "Enhancement of deep epileptiform activity in the EEG via 3-D adaptive spatial filtering," *IEEE Trans. Biomed. Eng.*, vol. 46, pp. 707-716, 1999.

[14] P. L. Nunez and R. Srinivasan, *Electric Fields of the Brain: The Neurophysics of EEG*, 2 ed. New York: Oxford University Press, 2006.

[15] V. Braitenburg and A. Schuz, *Cortex: Statistics and Geometry of Neuronal Connectivity*. Berlin: Springer-Verlag, 1991.

[16] B. D. Van Veen, W. van Drongelen, M. Yuchtman, and A. Suzuki, "Localization of brain electrical activity via linearly constrained minimum variance spatial filtering," *IEEE Trans. Biomed. Eng.*, vol. 44, pp. 867-880, 1997.

[17] K. Sekihara, S. S. Nagarajan, D. Poeppel, A. Marantz, and Y. Miyashita, "Application of an MEG eigenspace beamformer to reconstructing spatio-temporal activities of neural sources," *Hum. Brain Mapp.*, vol. 15, pp. 199-215, 2002.

[18] S. S. Dalal, J. M. Zumer, A. G. Guggisberg, M. Trumpis, D. D. Wong*, et al.*, "MEG/EEG source reconstruction, statistical evaluation, and visualization with NUTMEG," *Comput. Intell. Neurosci.*, vol. 2011, pp. 1-17, 2011.

[19] M. Diwakar, O. Tal, T. T. Liu, D. L. Harrington, R. Srinivasan*, et al.*, "Accurate reconstruction of temporal correlation for neuronal sources using the enhanced dual-core MEG beamformer," *NeuroImage*, vol. 56, pp. 1918-1928, 2011.